Registry No. H_2O, 7732-18-5; SiO_2, 7631-86-9.

References and Notes

(1) Walrafen, G. E.; Luck, W. A. P. In *Structure of water and aqueous solutions*; Luck, W. A. P., Ed.; Verlag Chemie: Weinham, 1974; p 222.

(2) Hadzi, D.; Bratoz, S. In *The Hydrogen Bond*; Schuster, P., Zundel, G., Sandorfy, C., Eds.; North Holland Publication: Amsterdam, 1976; pp 565, 613.

(3) Shivaglal, M. C.; Singh, S. *Int. J. Quantum Chem.* **1989,** *36,* 105.

(4) Brakaspathy, R.; Singh, S. *Chem. Phys. Lett.* **1986,** *131,* 394.

(5) Pelmenschikov, A. G.; Morosi, G.; Gamba, A. *J. Phys. Chem.* **1992,** *96,* 2241.

(6) Zhidomirov, G. M.; Kazansky, V. B. *Adv. Catal.* **1986,** *34,* 131.

(7) Ugliengo, P.; Saunders, V. R.; Garrone, E. *J. Phys. Chem.* **1990,** *94,* 2260.

(8) Hobza, P.; Sauer, J.; Morgeneyer, C.; Hurych, J.; Zahradnik, R. *J. Phys. Chem.* **1981,** *85,* 4061.

(9) Sauer, J.; Zahradnik, R. *Int. J. Quantum Chem.* **1984,** *26,* 793.

(10) Sauer, J.; Schroder, K.-P. *Chem. Phys. Lett.* **1984,** *107,* 530.

(11) Chakoumakos, B. C.; Gibbs, G. V. *J. Phys. Chem.* **1986,** *90,* 996.

(12) Sauer, J.; Schroder, K.-P. *Z. Phys. Chem. (Leipzig)* **1985,** *266,* 379.

(13) Peri, J. B.; Hensley, A. L. *J. Phys. Chem.* **1986,** *72,* 2926.

(14) Hertl, W.; Hair, M. L. *Nature* **1969,** *223,* 1950.

(15) Knozinger, H. In *The Hydrogen Bond*; Schuster, P., Zundel, G., Sandorfy, C., Eds.; North Holland Publication: Amsterdam, 1976; p 1263.

(16) Klier, K. *J. Chem. Phys.* **1973,** *58,* 737.

(17) Klier, K.; Shen, J. H.; Zettlemoyer, A. C. *J. Phys. Chem.* **1973,** *77,* 1458.

(18) Kazansky, V. B.; Gitscov, A. M.; Andreev, V. M.; Zhidomorov, G. M. *J. Mol. Catal.* **1978,** *4,* 135.

(19) Anderson, J. H.; Wickersheim, K. A. *Surf. Sci.* **1964,** *2,* 252.

(20) Zhdanov, S. P.; Kosheleva, C. S.; Titova, I. I. *Langmuir* **1987,** *3,* 960.

(21) Hoffman, P.; Knozinger, E. *Surf. Sci.* **1987,** *188,* 181.

(22) Fubini, B.; Bolis, V.; Giamello, E. *Inorg. Chim. Acta* **1987,** *138,* 193.

(23) Frisch, M. G.; Head-Gordon, M.; Schlegel, H. B.; Raghavachari, K.; Binkley, J. S.; Gonzales, C.; Defrees, D. J.; Fox, D. J.; Whiteside, R. A.; Seeger, R.; Melius, C. F.; Baker, J.; Martin, R.; Kahn, L. R.; Stewart, J. J. P.; Fluder, E. M.; Topiol, S.; Pople, J. A. *Gaussian*; Gaussian, Inc.: Pittsburgh, PA, 1988.

(24) Mix, H.; Sauer, J.; Schroder, K.-P.; Merkel, A. *Collect. Czech. Chem. Commun.* **1988,** *53,* 2191.

(25) Ugliengo, P.; Saunders, V. R.; Garrone, E. *J. Phys. Chem.* **1989,** *93,* 5210.

(26) Sauer, J. *J. Phys. Chem.* **1987,** *91,* 2315.

(27) Sauer, J. *Chem. Phys. Lett.* **1983,** *97,* 275.

(28) Sauer, J.; Morgeneyer, C.; Schroder, K.-P. *J. Phys. Chem.* **1984,** *88,* 6375.

(29) Ugliengo, P.; Garrone, E.; Ferrari, A. M.; Sauer, J.; Bleiber, A. *Proceedings of the 7th International Congress on Quantum Chemistry*, Menton, 1991; p 145.

(30) Pelmenschikov, A. G.; Paukshtis, E. A.; Zhanpeisov, N. U.; Pavlov, V. I.; Zhidomirov, G. M. *React. Kinet. Catal. Lett.* **1987,** *33,* 423.

(31) Paukshtis, E. A.; Pankratiev, Y. D.; Pelmenschikov, A. G.; Burgina, E. B.; Turkov, V. M.; Yurchenko, E. N.; Zhidomirov, G. M. *Kinet. Catal.* **1986,** *27,* 1440.

(32) Teunissen, E. H.; van Duijneveldt, F. B.; van Santen, R. A. *J. Phys. Chem.* **1992,** *96,* 366.

Phase Transitions in C60 and the Related Microstructure: A Study by Electron Diffraction and Electron Microscopy

G. Van Tendeloo,*,[†] C. Van Heurck,[†] J. Van Landuyt,[†] S. Amelinckx,[†] M. A. Verheijen,[‡] P. H. M. van Loosdrecht,[‡] and G. Meijer[‡]

Universiteit Antwerpen (RUCA) Groenenborgerlaan 171, B2020 Antwerp, Belgium, and Research Institute of Materials, University of Nijmegen, 6525 ED Nijmegen, The Netherlands (Received: February 19, 1992)

The phase transition in C60 and (related) lattice defects are studied by low-temperature electron microscopy and electron diffraction. The microstructure of the room-temperature face-centered-cubic (fcc-a_0) phase is very similar to that of a low stacking fault energy fcc alloy; micro twins and stacking faults on the {111} planes are the main defects. The phase transition fcc-a_0 ⟹ simple cubic (sc) at 249 K, is confirmed by single-crystal diffraction and the space group of the sc phase was unambiguously determined from the systematic extinctions as $Pa\overline{3}$. Moreover a second phase transition, sc ⟹ fcc-$2a_0$, is discovered. It occurs at a slightly lower temperature. It is suggested that in the sc phase the molecules still have a rotational degree of freedom about their respective ⟨111⟩ rotation axis, of which the orientation pattern is already fixed by the $Pa\overline{3}$ space group. In the fcc-$2a_0$ phase the rotation angle is found to be frozen in and to alternate between $+\varphi$ and $-\varphi$ along the ⟨100⟩ directions. The domain structure of the sc phase consists of eight variants (four translation variants for each of the two orientation variants) present in rather ill-defined regions. As a consequence of the ease of rotation of the molecules, no sharp interfaces are formed between different orientation domains.

1. Introduction

It seems by now well established that in the room-temperature phase of C60 the quasi-spherical molecules are packed in a face-centered cubic arrangement.[1–4] When the material is contaminated with residual solvent (e.g., toluene) or in the presence of a significant fraction of other fullerenes, such as C70, a faulted hexagonal phase may be stabilized at room temperature. However, when such material is moderately heated in the electron microscope vacuum, it transforms "in situ" into a somewhat faulted face-centered cubic arrangement.[4]

It has been demonstrated recently by the use of X-ray powder diffraction that below 249 K the lattice becomes primitive cubic. This transformation is attributed to the loss of orientational degrees of freedom of the C60 molecules on cooling below the transition temperature of 249 K.[5–8]

It is the purpose of this paper to confirm and complement these powder data by observations in the electron microscope on single-crystal specimens of high purity C60, as well as to discuss defects in the basic structure and in the low-temperature orientationally ordered phase. Moreover we shall demonstrate the existence of a second low-temperature phase which is face centered with a lattice parameter $2a_0$.

2. Crystal Production

The C60 crystals used in this study were prepared according to descriptions given in ref 9, whereby carbon soot is produced in a dc arc discharge between two high-purity graphite electrodes in a 0.2-atm He environment. Soxhlet extraction of this soot in boiling toluene is used to separate (mainly) C60 and C70 from the rest. This extract contains C60 and C70 in a 10:1 ratio, and this unseparated material is used in the experiments described in section 3.1.2; all other experiments were performed on pure crystals. Liquid column chromatography[10] is used to obtain C60 with a

---
[†] Universiteit Antwerpen.
[‡] Research Institute of Materials.
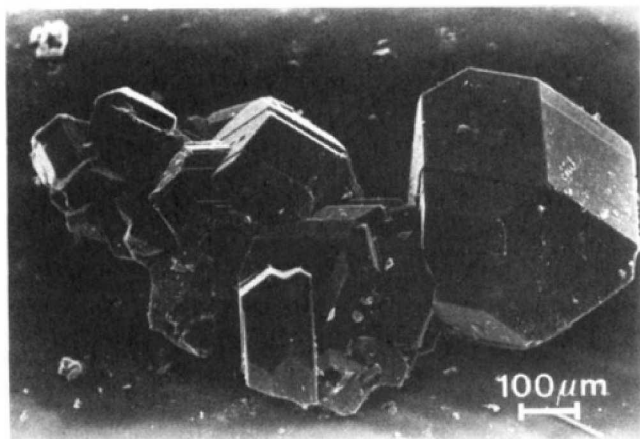
Figure 1. Scanning electron micrograph of single crystals of C_{60} obtained by vapor transport.

Figure 2. Electron diffraction patterns along different zones of a single crystal of C_{60} in the fcc phase: (a) [001] zone: the $h00$ spots are present as a result of double diffraction; (b) [011] zone, along this zone the rows of molecules are viewed along their densest direction; (c) [211] zone; (d) [111] zone, note the weak spots in the centers of the triangles of strong spots.

purity of at least 99.5%, as checked by mass spectrometry and NMR, and Raman spectroscopies. The C_{60} powder is washed with cyclohexane to remove any polyaromatic hydrocarbons that might still be present in the sample. About 10 mg of this C_{60} material is placed at the closed end of a 50-cm-long, 1-cm-diameter quartz tube with four necks at equal distances. The tube is evacuated to 10^{-5} Torr and heated to 250 °C for several hours to remove all the solvent that is embedded in the C_{60} minicrystallites that are formed after solvent evaporation of the chromatographically separated solution.
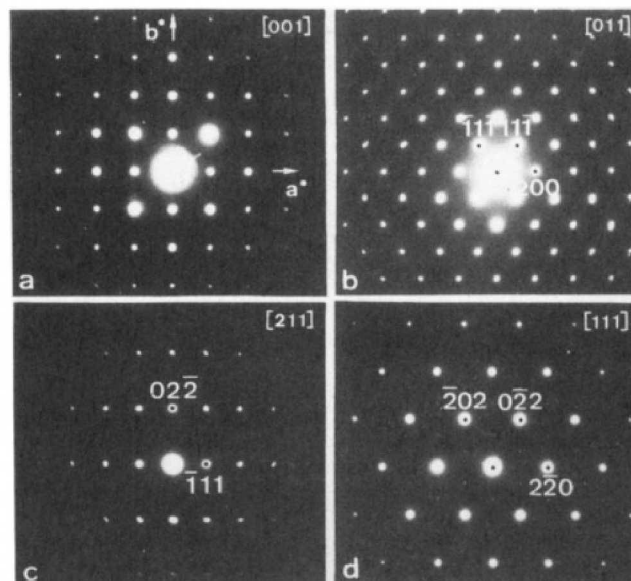
During all further heat treatments the quartz tube is kept at low pressure by continuous pumping. The end of the tube that contains the C_{60} powder is placed in a furnace and heated to 500 °C. The vapor pressure of C_{60} is strongly temperature dependent[11] and the sublimated C_{60} solidifies in the next section of the quartz tube, which is kept at a 100–150 °C lower temperature. Thus a large part of the C_{60} is vapor transported between two sections in approximately half an hour. Surprisingly, about one-third of the original material stays behind in the first section even after allowing vapor transport (at 500 °C) for several hours. Although both mass spectrometry and Raman spectroscopy seem to indicate that the material that stays behind is also C_{60}, we prefer not to use this material any longer as its vapor pressure is somewhat different. We therefore melt off the first segment of the tube and repeat the vapor transport two more times with the C_{60} material that did vapor transport the first time. Almost all of the latter material can easily be vapor transported into the fourth segment, which is subsequently sealed off on both sides. The isolated very pure C_{60} is then placed in a furnace kept at 500 °C for half an hour and cooled to room temperature in about 4 h. Beautiful C_{60} crystals as large as $0.5 \times 0.5 \times 0.5$ mm^3 are obtained in this way (Figure 1; see further details in ref 12).

Samples for electron microscopy were prepared by smoothly crushing the single crystals and dipping a copper grid, covered with glue, in the powdered material. Such crushing will break the single crystals but will hardly produce any dislocation structure or other crystal defects. Microscopy experiments were performed in a Philips CM 20 analytical electron microscope and a JEOL 4000 EX high-resolution microscope.

3. Observations

3.1. Room-Temperature Phase. *3.1.1. Electron Diffraction.* The electron diffraction patterns of a C_{60} high-purity single crystal in the room-temperature phase are characteristic of a face-centered cubic lattice with lattice parameter a_0, i.e., they exhibit only reflections for which the indices are either all odd or all even. However a quite remarkable feature is observed under the appropriate conditions; the $h00$ rows of reflections turn out to be completely absent or at least extremely weak. This was already noted in powder diffraction patterns by Heiney et al.;[6,13] we have confirmed this in our study by means of single-crystal diffraction experiments. By a careful tilting experiment, it could be shown that although the $h00$ rows of reflections are actually present

(Figure 2a), this is only because of double diffraction. Such unusual extinctions cannot be due to the presence of a particular combination of symmetry elements; it is accidental. A detailed explanation of the structural implications of these accidental extinctions is presented in a separate paper.[14] It is shown that this feature results from the absence along the ⟨100⟩ direction of periodicity in the scattering power. Due to a particular combination of the size of the spherical molecules and of the lattice parameter, the scattering power is very nearly constant in planes $h00$, $0k0$, and $00l$. In reciprocal space the Fourier transform of reasonable models for the spherical shell molecule has zero's at positions $h00$ for $h =$ even. This allows us to conclude that the molecules must behave as perfectly spherical shells of diffracting power, which is consistent with the assumption that they are freely rotating about their centre, without a preference for an instantaneous rotation axis.

The [111] zone diffraction patterns of certain crystal fragments exhibited some weak spots in the center of the triangles of intense spots (Figure 2d). Such spots are produced by streaks associated with planar disorder due to stacking faults, to twins, or to the presence of a small volume fraction of hexagonal phase.[4] However the diffraction patterns of most crystal fragments are free of such spots.

The presence in [110] zone diffraction patterns of strong streaks along the [1$\bar{1}$1] directions is sometimes noticed. More frequently these streaks exhibit reinforcements at the positions of split fcc spots; the splitting being $1/3$ of the interspot spacing along the [111]* direction. Every third [111] row remains unsplit. Such a diffraction pattern is the fingerprint of coherent (111) twins in the FCC structure. The frequent occurrence of twins usually correlates with a small value of the stacking fault energy, which is thus consistent with the occurrence of numerous stacking faults on (111) planes, causing the streaking (Figure 3).

3.1.2. High-Resolution Imaging. The perfect structure as imaged along the [111] zone is shown in Figure 4. The material used to produce these images contained about 10% of C_{70}, which is apparent from the different sizes of the bright dots that image the projected charge density produced by the columns of molecules. The bright areas correspond to channels in the structure (see ref 4 for more details). When molecules of a different size are present, the light areas in the image aquire a different size since the channels differ. Such local regions where C_{70} columns are present in a C_{60} matrix are indicated by arrows in Figure 4. The perfect structure as viewed along the [112] zone of the FCC structure
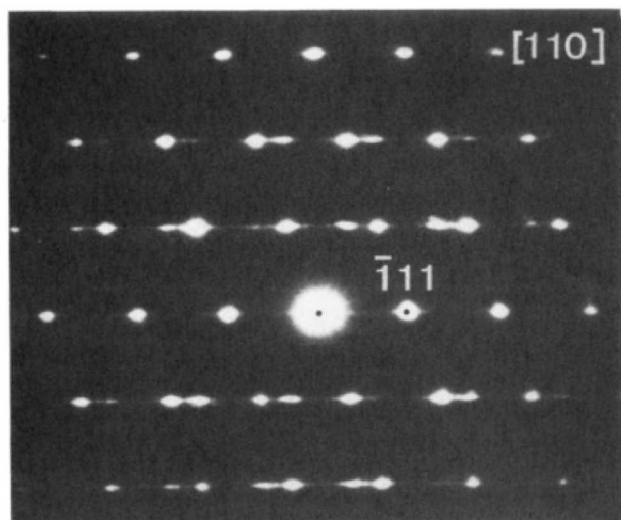
Figure 3. Electron diffraction pattern exhibiting fcc twin spots and streaks due to faulting on (111) planes.
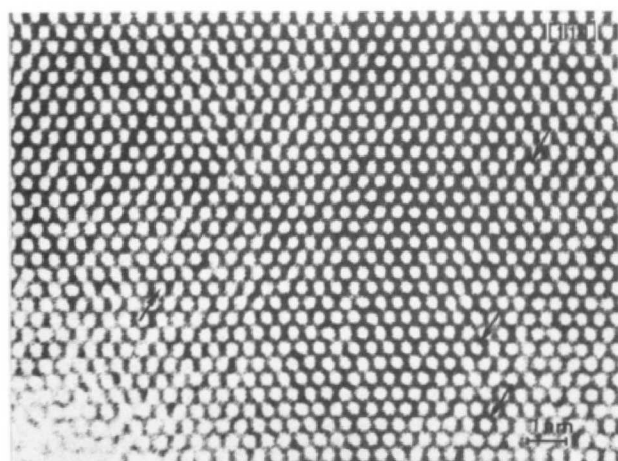

Figure 4. High-resolution image of C_{60} crystal containing 10% of C_{70} viewed along the [111] zone. Note the local differences in dot brightness attributed to the presence of C_{70} molecules.
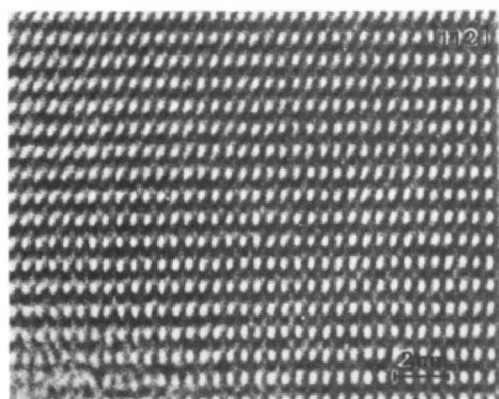

Figure 5. High-resolution image of high-purity C_{60} along the [112] zone. The molecular columns are imaged as black circular dots, the channels as bright elongated dots.

is reproduced in Figure 5. Along this zone the open channels in the FCC structure are elongated and have the geometry of the bright dots in Figure 5; circular dark dots represent columns of molecules. The interpretation of such images is thus straightforward if the foil is sufficiently thin. High-resolution images were also reported in refs 15–18 and scanning tunneling microscopic images in ref 19.

The geometry of the defects responsible for the streaking and for the twin spots in the diffraction patterns have been studied by means of high-resolution electron microscopy. The [110]* zone
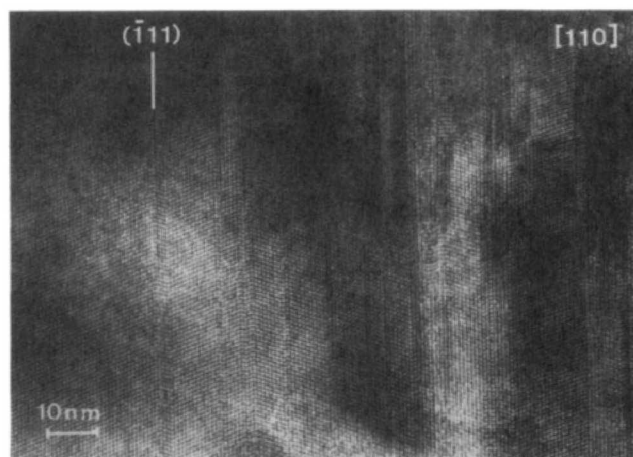
Figure 6. Microtwinned and faulted region of a crystal of C_{60}. The corresponding diffraction pattern is shown in Figure 3.
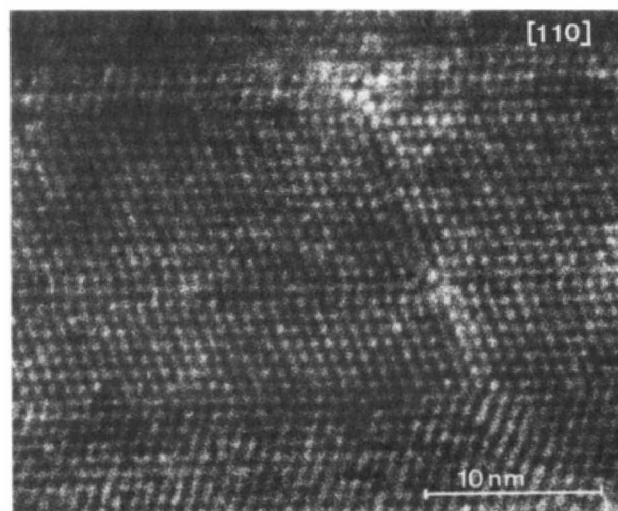
Figure 7. Intersecting stacking faults and twins in a crystal of C_{60} viewed along the [110] zone.

is the most informative one since it reveals directly the stacking of the densest packed rows of molecules. The crystals are found to contain most of the types of defects which commonly occur in the face centered cubic metals and alloys with low stacking fault energy; the most prominent feature in our samples being coherent microtwinning and stacking fault formation (Figure 6). Regions such as this one are responsible for the diffraction patterns such as Figure 3 containing streaks with reinforcements. Similar defects have been studied in refs 16–18.

An interesting and rather typical fault arrangement is shown in Figure 7. It consists of two intersecting stacking faults in {111} planes; one is ending in a coherent twin interface and causes a ledge in the twin interface (i.e., a twinning dislocation). It also causes a step in the intersected fault plane which is parallel to the coherent twin interface. Such an intersection line of stacking faults is equivalent to a row of fractional vacancies.[22]

The faults are of the intrinsic type ABCABABC, which implies that they could have been formed by the propagation of Shockley partials. The step in the horizontal fault suggests that this fault was formed first and was subsequently intersected by the other fault.

The similarity between the defects in C_{60} and in fcc-based alloys with low stacking fault energy is quite remarkable even though in the former case we have to do with van der Waals bonded molecules and in the latter case with atoms in metallic bonds. Both types of bonds are nondirectional however.

3.2. The Simple Cubic Structure. *3.2.1. Diffraction Patterns.* Low-temperature electron diffraction of C_{60} single-crystal specimens has confirmed the existence of a low-temperature phase based on a primitive cubic structure[6,20,8,21] and has allowed un-
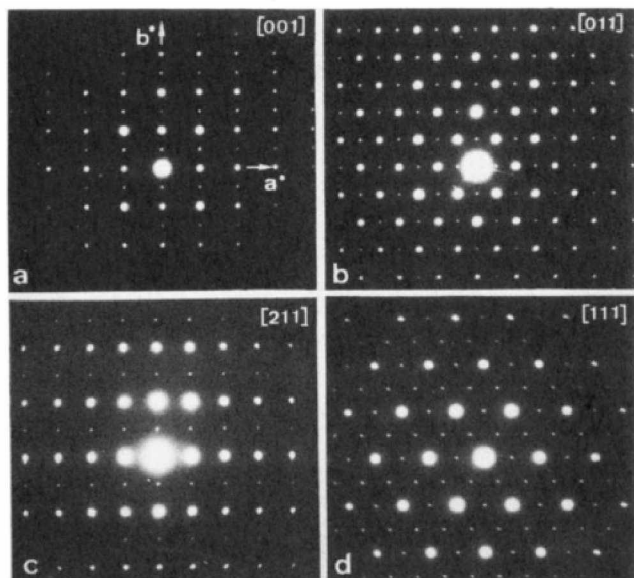
Figure 8. Electron diffraction patterns of the simple cubic phase along the same zones as in Figure 2 for the fcc zone: (a) [001] zone, note the presence of the $h00$ row with h = odd due to double diffraction, all reflections with k = odd are systematically absent; (b) [011] zone; (c) [211] zone; (d) [111] zone.

ambiguous confirmation of the space group as $Pa\bar{3}$.

On cooling the sample in the electron microscope below 249 K weak additional reflections appear in all zones. The most relevant sections of reciprocal space are shown in the sequence of diffraction patterns of Figure 8 obtained by tilting the same crystallite. It is quite obvious that the most intense spots still form a body-centered cubic lattice, i.e., the reciprocal lattice of a face-centered lattice. However, the weaker additional super-structure reflections occupy positions which are forbidden for a face-centered structure. All spots of this type can be indexed on the basis of a primitive unit cell with (approximately) the same lattice parameters as the face-centered cell. The following reflection conditions are clear from the (001)* section (Figure 8a): $0kl$ reflections are present for k = even. The $h00$ reflections h = odd are visible in most diffraction patterns but it could be shown by tilting experiments that they are formed by double diffraction. The reflection conditions thus have to be completed with: $h00$ reflections are present only for h = even. This set of diffraction conditions unambiguously identifies the space group as $Pa\bar{3}$, which confirms the suggestion made in a comment on ref 6 by Sachi-danandam and Harris,[20] after the initial structure determination was based on a different space group $Pn\bar{3}$.[6]

3.2.2. Structural Considerations. In the simple cubic (sc) structure the unit cell contains only one motive. This is only possible if the four sites of the fcc lattice become nonequivalent; we shall call the molecules occupying these sites respectively A, B, C, and D. The structure can now be described as consisting of four interpenetrating primitive lattices with the lattice parameters a_0, related by the lost symmetry translations, each being occupied by one type of molecule. It was shown in ref 6 that the A, B, C, and D molecules differ in their orientations and that the fcc–sc transition is an orientational order–disorder transition.

The orientations of the different molecules can be described as follows. In the reference orientation three mutually perpendicular binary axes of the molecule are parallel to the cube directions $\langle 100 \rangle$ of the lattice. The 3-fold axes of the molecule are then parallel to $\langle 111 \rangle$ directions of the lattice. In this orientation all molecules are equivalent and the lattice is still FCC. The symmetry is now broken by rotating the four different molecules A, B, C, and D about four different $\langle 111 \rangle$ directions over an angle φ.

The direction of the rotation axis and the senses of the rotations of the different molecules are of course related by the symmetry elements of the space group $Pa\bar{3}$. This is represented in Figure 9. The upper and lower ends of the bars, which are projections
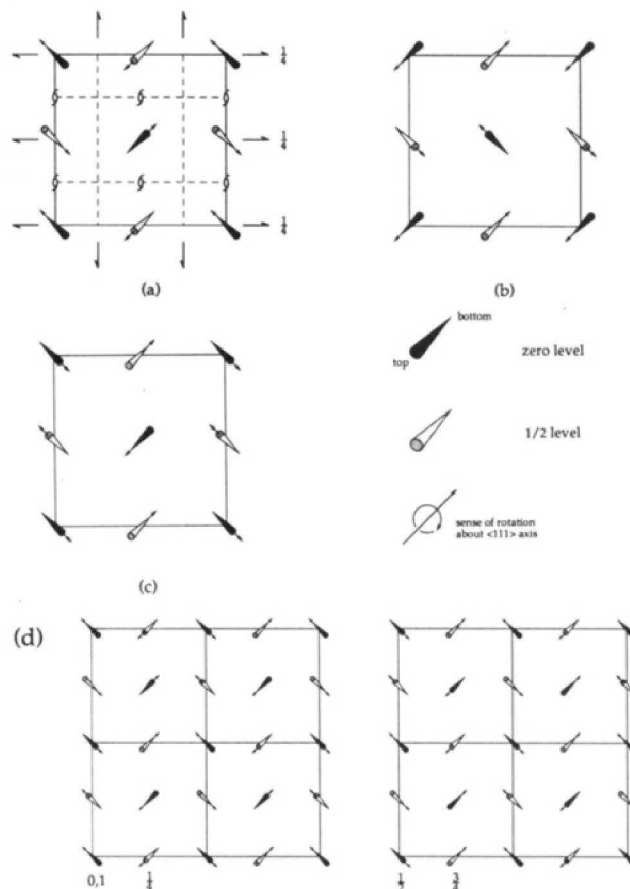
Figure 9. Schematic representation of orientationally ordered structures: (a) the sc structure, rotation angle $+\varphi$; (b) the 90° rotated structure of (a); (c) rotation angle has been changed from $-\varphi$ into $+\varphi$; (d) model for the fcc-$2a_0$ superstructure.

of $\langle 111 \rangle$ directions, indicate the sense of the inclinations. The arrow points indicate the sense of rotation over the angle φ. These two senses are not directly related since they transform differently under glide mirror operations. In Figure 9 the rotation sense of φ is defined as the sense in which a right-handed screw must be rotated in order to advance in the sense indicated by the arrow.

3.2.3. Structural Variants. The number of structural variants for a given choice of the angle φ can be found by considering separately the rotation and the translation variants.[23] The number of rotation variants is equal to the order of the point group of the high-temperature phase, which is 48, divided by the order of the point group of the low-temperature phase, which is 24. This yields two different orientation variants. These variants are related by one of the rotational symmetry operations lost during the transformation. In the present case the simplest choice is a rotation over 90° around one of the 2-fold axes of the pointgroup $m\bar{3}$, which is parallel to a cube direction. Since the point group of the sc phase contains a 3-fold axis, the three 2-fold axes are equivalent. The two orientation variants can thus be termed 90° rotation twins.

For each orientation variant four translation variants are possible, they are related by the fcc symmetry translations $[^1/_2\ ^1/_2\ 0]$, $[^1/_2\ 0\ ^1/_2]$, $[0\ ^1/_2\ ^1/_2]$, lost during the transformation. The total number of equally probable variants is thus 8. They are represented schematically in Figure 10.

It is also possible to consider directly the loss of space-group symmetry, which then leads directly to both types of structural variants. The order of the fcc space group is 192 and that of the $Pa\bar{3}$ spacegroup is 24, i.e., there are 192:24 = 8 variants.[24]

In a molecular crystal such as C_{60} still another type of structural variant, related to the orientation of the molecule itself, has to be considered. For such a highly symmetrical molecule the rotation angle can with the same probability be $+\varphi$ or $-\varphi$. The two structures in which the senses of the rotation angles differ are a priori equally probable and satisfy the same space group. It should
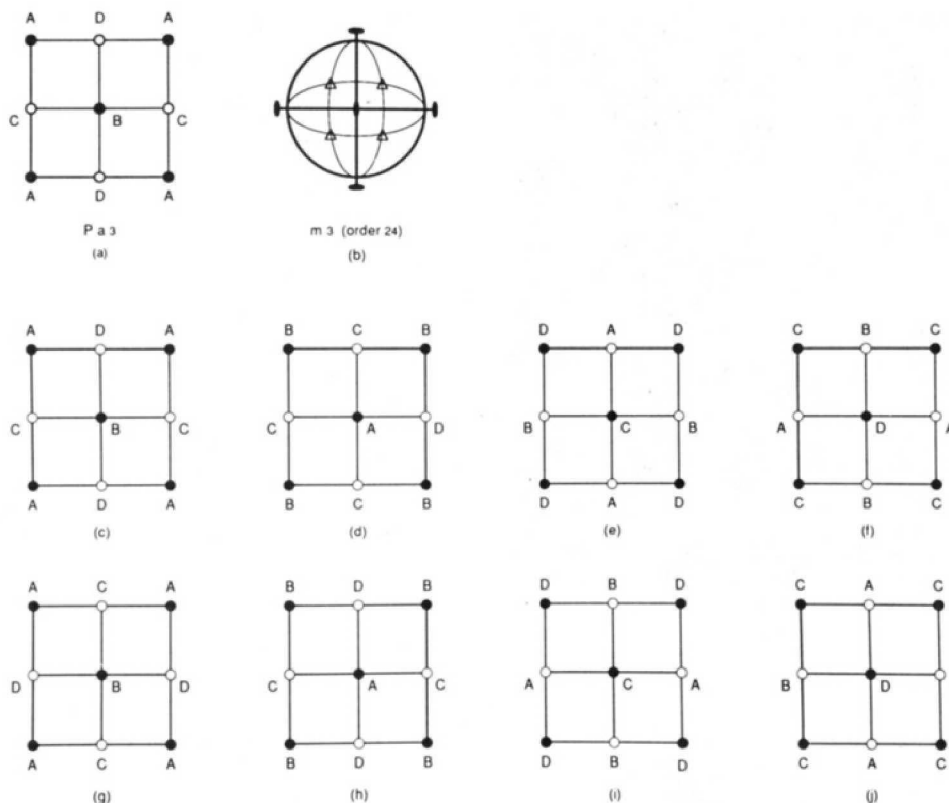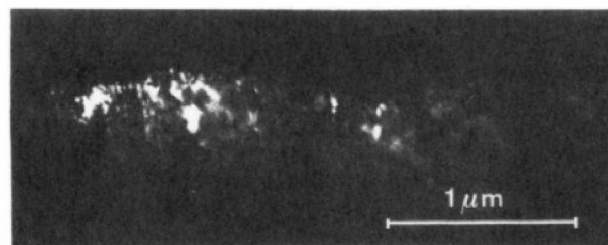
Figure 10. Schematic representation of different variants of the sc structure: (a) the sc structure; (b) symmetry elements of the point group *m*3; (c–f) translation variants of (a); (g–j) 90° rotation twins of the variants c–f, respectively. The capital letters represent molecules rotated over φ about different (111) axes.
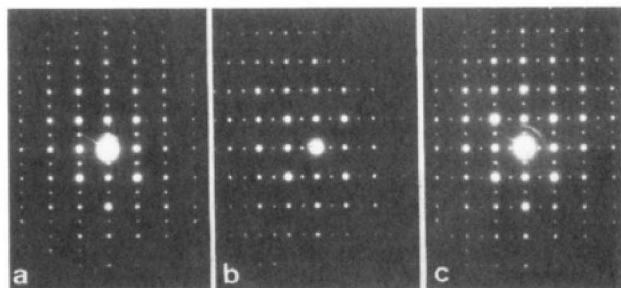
Figure 11. Diffraction patterns taken on both sides and across a 90° domain boundary: (a) to the left of the boundary; (b) to the right of the boundary; (c) across the boundary.

Figure 12. Dark-field image of the sc phase taken in a superstructure reflection, with the incident beam along the [001] direction.

be noted that the molecule as well as the structure contain a center of symmetry. The two structures are thus not enanthiomorphic and they are for instance *not* related by a mirror operation. The $+\varphi$ and $-\varphi$ structures are compared in Figure 9c.

3.2.4. Observation of Structural Variants. Although structural variants are generally easily observed, the imaging of structural variants in C_{60} turned out to be not straightforward. The 2-fold symmetry of the cube zone diffraction pattern provides a method to find diffraction evidence for the occurrence of relatively large 90° rotation domains. The experiment is illustrated in Figure 11. The specimen area producing the diffraction pattern of Figure 11a contains a single orientation domain. Shifting the selective aperture reveals the diffraction pattern of a neighbouring domain (see Figure 11b); it is rotated over 90° with respect to that of Figure 11a. On shifting the selector aperture, a 90° domain boundary was clearly crossed. Putting the selective aperture over the interface produces a pattern as in Figure 11c; it is the superposition of the two previous diffraction patterns. Moreover a weaker reflection is often visible in the centers of the squares. This spot is due to double diffraction originating from the areas where the two domains overlap. This could in principle be shown by making a dark field image in this double diffraction spot; only the region of overlap would then show up bright. This indicates

that the interfaces are inclined with respect to the incident beam, i.e., with respect to the cube orientations.

The standard method to reveal orientation variants is to make dark field images in reflections belonging to different variants (e.g., 120 and 210) of an area producing a diffraction pattern such as Figure 11c. The domains which produce intensity in the selected spot will then show up bright. Such experiments were repeatedly performed but failed to reveal well-defined domain walls; this is only partly due to the fact that the reflections are closely spaced and that the available objective apertures are unable to select a single reflection. Bright and dark patches were observed (Figure 12) but they were irregularly shaped and not bordered by sharp interfaces. The apparent absence of crystallographic interfaces is possibly related to the fact that the symmetry of the crystal lattice remains cubic on transformation. The discontinuous reduction in the length of the lattice parameter may lead to a fragmentation and to a roughening of the surface, but without the formation of crystallographically determined domain walls. In crystals which undergo a shape deformation of the lattice on transformation the domain walls are parallel to planes along which there is strain compatibility between two domains. However such strain-compatible planes are not defined if the transformation is accompanied by an isotropic contraction only.

The absence—in general—of sharp, well-defined domain interfaces is mainly to be related to the ease with which the spherical molecules are reorienting. Rather than forming a sharp interface
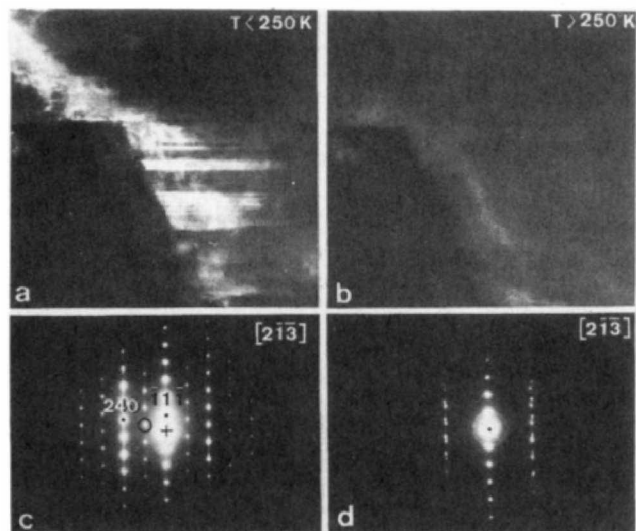
Figure 13. Diffraction experiment showing the relation between twin interfaces in the basic structure and orientation domain walls in the sc phase. (a) Dark-field image at liquid nitrogen temperature in a 120 superstructure spot surrounded by a small circle in the corresponding diffraction pattern (c). (b) Dark-field image under the same diffraction conditions above the 250 K transition. In the corresponding diffraction pattern at room temperature (d) all superstructure reflections have disappeared.

Figure 14. Diffraction pattern along the [110] zone exhibiting streaks along [111] through basic spots as well as through superstructure spots due to the SC structure.

Figure 15. Diffraction pattern along the [011] zone taken at liquid nitrogen temperature. Note the weak superstructure spots due to the fcc-2a$_0$ phase. The sc-a$_0$ structure reflections have been surrounded.
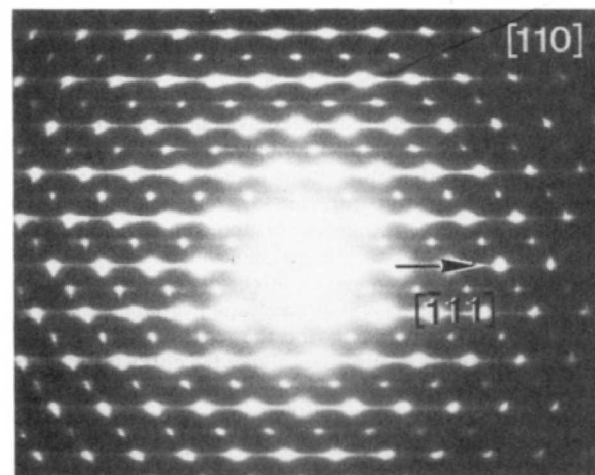
along which the pattern of rotation axis would change abruptly, the molecules can gradually rotate from the orientation they have in one domain to that in the other domain, hereby forming a transition layer with a certain width.

Whereas in unfaulted parts of the crystal the domains are isometric but irregular in shape and the boundaries ill-defined and noncrystallographic, this is no longer the case if twin boundaries or stacking faults are inherited from the basic structure. The presence of such boundaries in the basic structure apparently induces a change in the orientation pattern of the molecules which causes these boundaries to become also domain boundaries of the orientationally ordered superstructure. However this is not invariably the case, certain boundaries are apparently more effective than others in doing so.

Figure 13 shows an experiment illustrating this point. In Figure 13a the sample is in the orientationally ordered phase, as is apparent from the corresponding [2$\bar{1}$3]* type diffraction pattern of Figure 13c. The image of Figure 13a is formed using a 120 superstructure reflection, which is encircled in Figure 13c. It is clear that bright and dark bands are present which are limited by planar defects along (111) planes. One could at fist sight interpret this banded contrast as being due to the presence of twins in the basic structure; however, imaging is performed in a superstructure reflection. Moreover when the sample is heated above the transformation temperature of 250 K, without changing the diffraction conditions, all contrast disappears, even though the lattice defects remain (see Figure 13b). The corresponding diffraction pattern is reproduced in Figure 13d; superstructure reflections are no longer visible. Since no active reflection is selected under these conditions the image is formed by inelastically scattered electrons. This experiment is consistent with the interpretation of the bright areas as ordered domains of the selected variant.

The proposed relationship between faults and domain walls is further suggested by the diffraction pattern of Figure 14 taken at low temperature. It shows that a faulted region of the basic structure, as revealed by the streaks through the basic spots, is transformed into a region of the ordered phase, which is faulted on the same (111) planes, as judged from the streaks through the superstructure spots. The experiment is not completely conclusive since double diffraction, out of the streaks in the basic structure, might contribute to streaks through the superstructure spots.

3.3. The Low-Temperature Structure. *3.3.1. Diffraction Evidence.* Careful examination of diffraction patterns of specimens
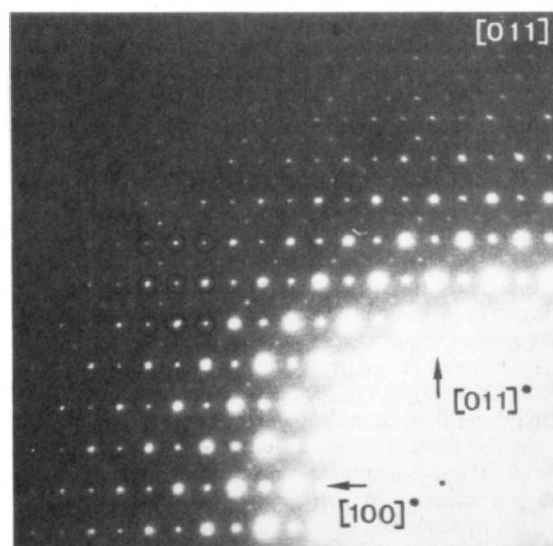
cooled to liquid nitrogen temperature revealed the presence of weak reflections which are not consistent with a simple cubic (sc) structure. In particular in the [110]$^{\bullet}$ section of reciprocal space the rectangular meshes are centered by weak but unambiguously identifiable spots (Figure 15). It was carefully verified that these spots could not be due to spikes coming from higher level zones in the reciprocal space of the simple cubic structure; they are also not compatible with reflections introduced by twinning or faulting in the basic structure.

It is worth noting that these weak spots become, relative to the basic and the superstructure spots, more intense with increasing length of the diffraction vector. This is a characteristic feature of periodic displacement modulated structures. Such displacements can for instance be caused by a finite rotation of the molecule around an axis.

The relative weakness of the supplementary reflections indicates that the superstructure presumably does not deviate very much from the simple cubic, orientationally ordered structure; which is described above and which was shown to account satisfactorily for the intensities of the observed X-ray powder diffraction patterns.[6,8] Also the single-crystal X-ray measurements by Liu et al. at 110 K failed to detect this superstructure.[21]

3.3.2. Model. Bearing in mind the last remark of the previous paragraph, we propose a model for this superstructure which involves the least changes with respect to the model for the simple cubic structure. We retain the configuration of rotation axes, but

in order to double the lattice parameters we assume that along the $\langle 100 \rangle$ rows the molecules are alternatingly rotated over an angle $+\varphi$ and $-\varphi$. This model is represented schematically in Figure 9d together with the configuration in the simple cubic phase. In this way orientationally equivalent molecules are dispersed as uniformly as possible throughout the structure. Molecules of a given orientation form a face centered cubic arrangement with a lattice parameter $2a_0$. The structure consists of eight such interpenetrating face-centered cubic lattices; each occupied by a given type of oriented molecule. A single crystal of such material will presumably be fragmented in a large number of variants, translation as well as orientation variants, due to the orientation of the rotation axis and the sense of rotation of the molecules in the different sublattices. Since the diffraction patterns of the different variants produce coincident spots, this will not be apparent from the electron diffraction pattern.

4. Conclusions

In our view the main results of this electron microscopy and diffraction study is the discovery that an orientationally ordered face-centered cubic structure with a double lattice parameter $2a_0$ occurs at liquid nitrogen temperature. From our observations we cannot conclude whether the new phase is formed at a higher or at a lower temperature than the simple cubic phase. However since temperature lowering usually leads to the loss of symmetry, we are inclined to believe that the $2a_0$-fcc phase presumably occurs at a slightly lower temperature than the simple cubic phase. The evidence from differential scanning calorimetry measurements[25] suggests that two transitions occur at temperatures which do not differ very much around 249 K.

With decreasing temperature the first to occur would thus be the transition from fcc-a_0 to a simple cubic structure. We speculate that in this phase the rotation axis of the molecules are fixed, according to the scheme proposed in ref 6 but that the molecules still have a rotational degree of freedom about their axis and, for instance, librate in an incorrelated way between two values $+\varphi$ and $-\varphi$; on the average all molecules with the same $\langle 111 \rangle$ rotation axis would then still be equivalent and the structure could be simple cubic. In the literature two different values of φ have been suggested for the sc structure, as deduced from neutron scattering.[6] In ref 4 φ is taken as $26°$, but in ref 8 $\varphi = 98°$. This can be rationalized by assuming that the sum of the two angles ought to be $120°$ rather than $124°$. Since a $120°$ rotation is a symmetry operation of the molecule, the two structures would then in fact be closely equivalent.

We believe that at somewhat lower temperature a $2a_0$-fcc structure is formed, whereby the molecules adopt well-defined orientations, alternatingly rotated over $+\varphi$ and $-\varphi$ along the $\langle 100 \rangle$ directions, about their respective axis.

The occurrence of more than one orientational phase transition is in line with the recent theoretical predictions by Michel.[26]

A second surprising observation in the present study was the difficulty of revealing a well-defined domain structure, which should undoubtedly be present. We believe that the main reason

for this is the ease with which the molecules reorient, even in the sc phase. Rather than abruptly changing their rotation axis, or rotation angle, along sharp interfaces, the molecules change gradually in orientation, giving rise to ill-defined curved interfaces.

References and Notes

(1) Fleming, R. M.; Siegrist, T.; Marsh, P. M.; Hessen, B.; Kortan, A. R.; Murphy, D. W.; Haddon, R. C.; Tycko, R.; Dabbagh, G.; Mujsce, A. M.; Kaplan, M. L.; Zahurac, S. M. *Mater. Res. Soc. Symp. Proc.* **1991**, *206*, 691.

(2) Smalley, R. E. "The almost (but never quite) complete Buckminsterfullerene bibliography"; available on request from: "Buckybib", Department of Chemistry, Rice University, PO Box 1892, Houston, TX 77251.

(3) Huffman, D. *Phys. Today* **1991**, *Nov*, 22.

(4) Van Tendeloo, G.; Op de Beeck, M.; Amelinckx, S.; Bohr, J.; Krätschmer, W. *Europhys. Lett.* **1991**, *15*, 295.

(5) Dworkin, A.; et al. *C. R. Acad. Sci. Paris Ser. II* **1991**, *312*, 665.

(6) Heiney, P. A.; Fisher, J. E.; Mc Ghie, A. R.; Romanow, W. J.; Denenstein, A. M.; Mc Cauley, Jr., J. P.; Smith, III, A. B.; Cox, D. E. *Phys. Rev. Lett.* **1991**, *66*, 2911.

(7) Neumann, D. A. *Phys. Rev. Lett.* **1991**, *67*, 3808.

(8) David, W. I. F.; Ibberson, R. M.; Matthewman, J. C.; Prassides, K.; Dennis, T. J. S.; Hare, J. P.; Kroto, H. W.; Taylor, R.; Walton, D. R. M. *Nature* **1991**, *353*, 147.

(9) Krätschmer, W.; Lamb, L. D.; Fostiropoulos, F.; Huffman, D. R. *Nature* **1990**, *347*, 354.

(10) Aije, H.; Alvarez, M. M.; Anz, S. J.; Beck, R. K.; Diederich, F.; Fostiropoulos, K.; Huffman, D. R.; Krätschmer, W.; Rubin, Y.; Shriver, K. E.; Sensharma, D.; Whetten, R. L. *J. Phys. Chem.* **1990**, *94*, S630.

(11) Pan, C.; Sampson, M. P.; Chai, Y.; Hague, C. R.; Margrave, J. L. *J. Phys. Chem.* **1991**, *95*, 2944.

(12) Verheijen, M. A.; Meekes, H.; Meijer, G.; Raas, E.; Bennema, P. *Chem. Phys. Lett.* **1992**, *191*, 339.

(13) Heiney, P. A.; et al., submitted to *Phys. Rev. B, Rapid Commun.*

(14) Amelinckx, S.; Van Heurck, C.; Van Dyck, D.; Van Tendeloo, G. *Phys. Status Solidi* **1992**, *131*, 589.

(15) Dravid, V. P.; Liu, S.; Kappes, M. M. *Chem. Phys. Lett.* **1991**, *185*, 75.

(16) Disko, M. M.; Behal, S. K.; Sherwood, R. D.; Cosandey, F.; Lu, P.; Creegan, K. M.; Tindell, P.; Cox, D. M. Proceedings of the 49th Annual Meeting of the Electron Microscopy Society of America; Bailey, G. W., Ed.; San Francisco Press, Inc.: San Francisco, 1991; p 1024.

(17) Wang, S.; Buseck, P. R. *Chem. Phys. Lett.* **1991**, *182*, 1.

(18) Luzzi, D. E.; Fischer, J. E.; Wang, X. Q.; Ricketts-Foot, D. A.; Mc Ghie, A. R.; Romanow, W. J. *J. Mater. Res.*, in press.

(19) Wilson, R. J.; Meijer, G.; Bethune, D. S.; Johnson, R. D.; Chambliss, D. D.; de Vries, M. S.; Hunziker, H. E.; Wendt, H. R. *Nature* **1991**, *348*, 621.

(20) Sachidanandam, R.; Harris, A. B. *Phys. Rev. Lett.* **1991**, *67*, 1467.

(21) Liu, S.; Lu, Y.-J.; Kappes, M. M.; Ibers, J. A. *Science* **1991**, *254*, 408.

(22) Amelinckx, S. *Dislocat. Solids* **1979**, *2*, 144.

(23) Van Tendeloo, G.; Amelinckx, S. *Acta Crystallogr.* **1974**, *A30*, 431.

(24) Gratias, D.; Portier, R. In *Microscopie Electronique en Science des Matériaux, 1981*; Jouffrey, B., Bourret, A., Colliex, C., Eds.; CNRS Editions: 1983; p 229.

(25) Samara, G. A.; et al. *Phys. Rev. Lett.* **1991**, *67*, 3136.

(26) Michel, K. H. *Chem. Phys. Lett.* **1992**, *193*, 478.